

# Towards a model of dry shear keyed joints: modelling of panel tests

J. Turmo\*, G. Ramos and A.C. Aparicio

*Department of Construction Engineering, Universitat Politècnica de Catalunya,  
Barcelona Tech. c/Jordi Girona 1-3, C1, 08034. Barcelona, Spain*

*(Received December 10, 2009, Revised April 10, 2012, Accepted May 18, 2012)*

**Abstract.** This paper presents a study on the behaviour of the joints of segmental concrete bridges with external prestressing, focusing on the structural response of dry non-epoxied joints with shear keys. A Finite Element joint model to study such structures is validated modelling eight concrete panel tests. The most important feature of this model is that it has been validated with experimental tests on concrete panels which were specifically designed to fail in shear. Interface elements are used to reproduce the non linear behaviour of the joint and parameters deduced from the tests are used to define the constitutive law of these elements. This joint model is of great importance because it will permit the development of a structural model that faithfully reproduces the behaviour of these structures under combined flexure and shear and the study of its global behaviour after the opening of the joints. Interesting conclusions about the behaviour of the dry joints, about the contribution of the different mechanisms transferring shear (friction and cohesion) and about the shear stress distribution in the joint have been reached.

**Keywords:** segmental bridges; castellated joints; shear strength; dry joints; shear keys.

---

## 1. Introduction

Prefabricated segmental concrete bridges with external prestressing and dry joints are associated with a span-by-span construction process that is thought to be the fastest of its type. For the construction of each of the spans, the segments are placed one next to the other, suspended from a beam or arranged in a mobile falsework, and are assembled by means of external prestressing. In Europe, where usually a waterproofing layer to prevent leakage is applied on the top of the deck, it is not necessary to apply any epoxy resin between the joint-faces of the segments. It is precisely the subject matter of the present work to study externally prestressed segmental bridges with resin-free dry joints. Its most significant characteristic is the nonexistence of bond reinforcement crossing the joints, neither active nor passive. The first constructed example of such a structure was the Long Key Bridge (Muller 1980). A more recent well documented example can be found in Bangkok (Brockmann and Rogenhofer 2000).

Even though the use of dry joints is still a common practice in many countries in Europe and Asia, in the United States, it is not allowed anymore (AASHTO 2010). It was eliminated from AASHTO specifications in the 2003 revision due to the critical nature of post-tensioning reinforcing and the need for a multiple layer protection system. Failures of some post-tensioning reinforcing in

---

\* Corresponding author, Professor, E-mail: [jose.turmo@upc.edu](mailto:jose.turmo@upc.edu)

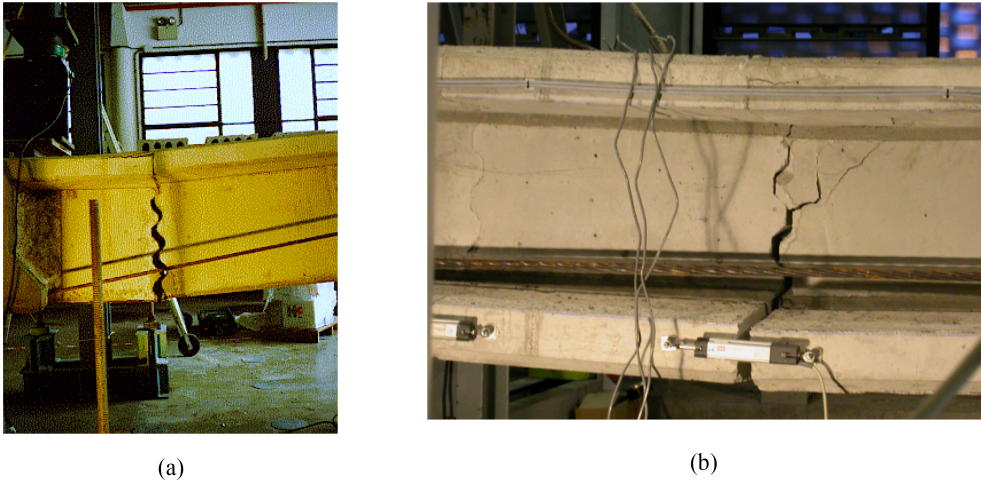


Fig. 1 Beam tests. Open Joint at ULS: (a) Flexural failure and (b) shear failure (Turmo 2003)

Florida and Europe due to corrosion have resulted in a review of the effectiveness of previous multiple layer protection systems.

Due to the fact of not having any bonding reinforcement crossing the joints, these structures have a significantly different behaviour than regular unbounded prestressed concrete beams (Au *et al.* 2009). Moreover, such joints represent a weak point for actual structures (Kamaitis 2008, Rombach GA and Abende 2008). Hence, prestressing design is accomplished in such a manner that the limit state of decompression of the joints is not surpassed in Service Limit State (SLS). When the load increases beyond the Ultimate Limit State (ULS), the joints open ostensibly (Fig. 1); the structure rapidly loses stiffness, and reaches a considerable deflection. Due to the important opening of the joint, the arrangement of some castellated keys in the joint is mandatory to facilitate the transference of shear after decompression. In this manner, the shear stresses are transmitted across the joint through two different mechanisms. The first mechanism represents the friction resistance that arises when two flat and compressed surfaces attempt to slide one against the other, whose resistance is proportional to the actuating compression and the corresponding proportionality factor is called friction coefficient,  $\mu_1$ . The second mechanism considers the support effect of the castellated shear keys in contact. These keys permit the shear transfer behaving like small plain concrete corbels (the small dimensions of the keys do not permit to place conventional reinforcement). The shear strength of the keys by surface area is called cohesion,  $c$ . If compression stresses,  $\sigma_n$ , exist, then the keys turn to be small prestressed concrete corbels, increasing the ultimate shear capacity with compression. The corresponding proportionality factor is called internal friction,  $\mu_2$ . This behavior has been checked empirically for both epoxy-glued and non epoxy-glued joints (Ramirez *et al.* 1993, Buyukozturk *et al.* 1990, Rombach and Specker 2000, Megally *et al.* 2003a, 2003b, Zhou *et al.* 2005, Issa 2007). It is to highlight that epoxy glued joint shear strength is always higher than of those unepoxied, the epoxy in the joint decreasing the effect of the fitting imperfections between the match cast segments.

Hence, a dry joint is certainly a physical and geometrical discontinuity, since it can not resist tensile stresses and there is no bonded reinforcement to control its opening. Several researchers have numerically reproduced this discontinuity and modelled the behaviour of these structures in flexure

(Ramos and Aparicio 1996, Muller and Gauthier 1990, Naaman 1990, Rezendre 1989, Vonganan 1997, Rombach and Specker 2000). However, numerical studies on the behaviour of these structures under a combination of normal stresses (axial and flexural loads) and tangential stresses (shear and torsion) are much more limited (Huang and Eibl 1993, Rombach and Specker 1999, Rombach 2004).

Huang and Eibl (1993) studied the behaviour of simply supported and continuous segmental bridges with dry joints, modelling the behaviour under flexure, shear and torsion through the finite element program ABAQUS. They firstly carried out a Finite Element Method (FEM) analysis that included a nonlinear geometrical behaviour and a linear-elastic material constitutive law. Flanges and webs of the girder were modelled by plate elements (analysis in 3D with 2D elements). The joints were modelled by special contact elements allowed to transmit compression and tangential stresses when the elements were in contact. The keys were not geometrically modelled. The results obtained in this first analysis were applied to an individual segment in a second analysis considering the nonlinear material behaviour.

Rombach and Specker (Rombach and Specker 1999, Rombach 2004), numerically studied the behaviour of simply supported and continuous segmental bridges. To calibrate the model, these authors used the response of a real scale test carried out on a real span of the “Second Stage Expressway System”, which was tested up to failure in Bangkok (Takebayashi *et al.* 1994). The test was modelled with three-dimensional finite elements. The keys were modelled with their actual geometry and the opening of the dry joints was obtained using interface elements. Once calibrated, the model was used to reproduce the behaviour of this type of bridges under combined flexure, shear and torsion. Different support conditions were taken into account. The principal advantage of modelling the joints with their real geometry is to permit the shear transfer in spite of the fact that the joints are opened.

In this paper, a joint model is presented to study shear transfer between non epoxy dry match cast joints with shear keys between concrete segments. The results presented in this paper are part of a larger research project on the shear transfer of externally prestressed precast segmental bridges. In this frame, some other actions not presented in this paper were undertaken: (1) eight panels were tested under shear up to failure (Turmo *et al.* 2006a), (2) six beams were tested under flexure and shear (Turmo *et al.* 2006b), (3) beam tests were modelled and conclusions about the mechanism resisting coupled shear and bending in such beams were reached (Turmo *et al.* 2006c), (4) simply supported segmental concrete bridges with external prestressing and dry joint were studied and design conclusions were drawn (Turmo *et al.* 2005) and (5) continuous bridges were also investigated and design conclusions were drawn (Turmo *et al.* 2011).

The joint model presented in this paper has been validated with shear tests performed on eight concrete panels. This experimental program was carried out at the Laboratory Luis Agullo of the Department of Construction Engineering, at the Universitat Politècnica de Catalunya (UPC) (Turmo *et al.* 2006a). The most important feature of this model is that it has been validated with experimental tests on concrete panels which were specifically designed to fail in shear. Other models have not been calibrated, or have been calibrated with tests where the elements failed under flexure. In the opinion of the authors, this joint model is of great importance because it permits the development of a structural model that faithfully reproduces the behaviour of these structures under combined flexure and shear and the study of its global behaviour after the opening of the joints. Herein, interesting conclusions have been reached regarding the behaviour of dry joints and the different mechanisms of shear transfer of such joints.

## 2. Brief description of the tests used for the validation of the model

This section presents a brief description of the tests carried out to validate the numerical model, emphasizing on the most important details for the modelling. An exhaustive description of the test development and results can be found in Turmo *et al.* (2006a).

Panel tests consisted in two series of four panels each: one series was cast with conventional concrete (PC), and the other with steel fibre reinforced concrete (SFRC). There were three objectives to achieve: (1) to evaluate the load-carrying capacity of a dry joint, (2) to study the strength increase when providing shear keys in a smooth joint and (3) to compare the behaviour of PC and SFRC joints. It is to highlight that the possibility of increasing the toughness and strength of the unreinforced keys by using SFRC was first tested at Massachusetts Institute of Technology (MIT) (Beattie *et al.* 1989, Buyukozturk *et al.* 1990). Each panel setup consists in three sub-panels of 0.1 m thick assembled with prestressing bars. The geometry of the joints as well as the prestressing force varied as a function of the specific objective of the tests. Hence, the following four joint conditions were studied, covering from smooth flat joints to joints with multiple keys:

(1) Friction test (PC-R and SFRC-R): The joints between the subpanels are flat, without keys. Thus, the only mechanism to develop shear resistance is friction. The objective of this test is to determine the concrete-to-concrete friction coefficient of the joint,  $\mu_1$ , and study its evolution as the contact surfaces deteriorate.

(2) Cohesion test (PC-C and SFRC-C): The joints between subpanels have 7 keys. A certain separation was maintained between the faces of the subpanels (around the 10% of the key length). In this manner, no shear resistance due to friction is developed. On the other hand, to avoid the transmission of normal forces by the keys, neoprene-teflon sheets were placed at the top and bottom of the joints. In this way, contact between keys occurred only after loading began. The objective of this test is to determine the cohesion component,  $c$ , since there are no normal stresses in the key zone.

(3) Combined test with closed joints (PC-JC and SFRC-JC): The joints between subpanels have 4 keys and the faces of the subpanels are in contact. The prestressing of the panel maintains the joints closed when loading is applied. The objective of this test is to determine the load-carrying capacity of the joint before reaching the limit state of decompression.

(4) Combined test with open joints (PC-JA and SFRC-JA): The joints between subpanels have 7 keys and the faces of the joint are in contact. In this case, the segments are maintained together with passive bars, with no initial prestressing force. Then, the joints will open when loading is applied. The objective of this test is to determine how does the cinematic of the joint affect the shear force that it is capable to transfer, verifying up to what extent the keys that are under the neutral axis contribute to the shear resistance. This test aims to reproduce the behavior of the joints of segmental bridges without bond reinforcement, in which the joints open ostensibly.

All the panels were tested under shear using a MTS testing system under displacement control. All tests were taken up to complete failure, which always occurred in the section of the joint. The outline of the tests with the corresponding nomenclature is presented in Table 1.

In Fig. 2, the load-deflection diagrams for all these tests are depicted. Comparing the tests, two by two, it can be checked that PC and SFRC panels behaved in a very similar manner during the tests and their shear strength was also similar. Hence, material shows little influence on the pre-peak behaviour of the panels.

The failure mode observed on panels is radically different than that observed in experimental tests

Table 1 Test program. UPC panels

Test	Joint type	Shear transfer	Material
PC-R	No shear keys.	$\mu_1$	PC
PC-C	Shear keys. Gap between panels.	$c$	PC
PC-JC	Shear keys. Closed joint.	$\mu_1, \mu_2, c$	PC
PC-JA.	Shear keys. Open joint.	$\mu_1, \mu_2, c$	PC
SFRC-R	No shear keys.	$\mu_1$	SFRC
SFRC-C	Shear keys. Gap between panels.	$c$	SFRC
SFRC-JC	Shear keys. Closed joint.	$\mu_1, \mu_2, c$	SFRC
SFRC-JA.	Shear keys. Open joint.	$\mu_1, \mu_2, c$	SFRC

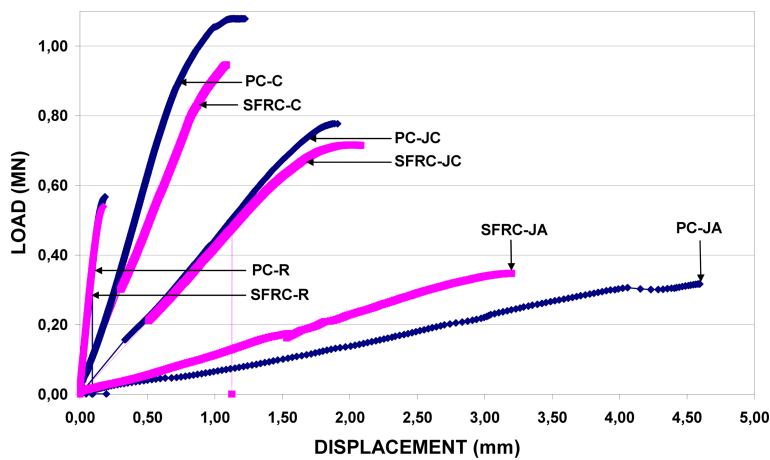


Fig. 2 Load-deflection diagrams of the experimental tests

on scaled girders. In the case of panels, cracking is vertical and the keys fail in the plane of the joint. In the case of girders, it is a diagonal cracking that induces failure, starting at the joint and progressing across the segment (Fig. 1b). During beam tests (Ramirez 1989, Aparicio *et al.* 2001, Turmo *et al.* 2006b), the joint presents an elastic behaviour and the keys maintain their integrity during failure.

### 3. FEM analysis of the panels

#### 3.1 Modelling of the joints

There is a frictional type of behaviour between the faces of the joint. The singular nature of the union between sub-panels is modelled by interface elements as this shown in Fig. 3. The constitutive law of these interface elements was a Coulombian type friction law, without cohesion (Fig. 4). Then, the yield surface  $f$ , or the state of stress beyond which yielding starts, is defined by Eq. (1)

$$f = \sqrt{t_t^2 + t_n} \cdot \tan \phi = 0 \quad (1)$$

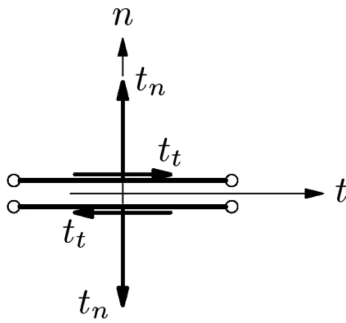


Fig. 3 Interface element

Table 2 Constant values adopted to model a concrete dry joint

$k_n$	$10^7 \text{ MN/m}^3$
$k_t$	$10^7 \text{ MN/m}^3$
$\tan \phi$	0,55
$\tan \varphi$	0,0

and the potential yield surface  $g$ , which governs the behaviour of the joint after yielding, by Eq. (2)

$$g = \sqrt{t_t^2} + t_n \cdot \tan \phi = 0 \tag{2}$$

Important penalty values were assigned to the normal and tangential stiffness coefficients ( $k_n$  and  $k_t$ ), that relate the normal and tangential stresses of the joint ( $t_n$  and  $t_t$ ) in the elastic state to the relative normal and tangential displacements between the joint faces ( $\Delta u_n$  y  $u_t$ ). These penalty values intend to simulate the initial continuous geometry before the decompression. In the elastic state, the normal and tangential behaviours of the joint are decoupled.

The values adopted for the characterization of the joint are shown in Table 2. The value of  $\tan \phi$  is taken equal to the friction coefficient between two concrete surfaces,  $\mu_1$ , measured in experimental tests (Turmo 2006a), so that the maximum tangential stress that the joint is able to transmit is  $\tau_u = t_t = t_n \tan \phi = t_n \mu_1$ . The value adopted for  $k_t$  assures that the relative displacement between the faces of the joint does not surpass 0.001 mm for a shear stress of 10 MPa. The cohesion value is equal to zero. Then, if the joint is not compressed, it is not capable of transmitting neither tensile nor shear stresses. Once the maximum shear stress is reached, the faces of the joints slide. The value of the angle  $\varphi$ , or dilatancy angle, is taken equal to zero. When the limit state of decompression is reached, ( $t_n=0$ , apex of the yielding surface in Fig. 4), the displacement between both sides of the joint are not directly linked anymore.

The considerations of the previous paragraph are valid for the modelling of the neoprene-teflon sheets that were interposed between the faces of the joints in tests C and JC. In this case, the concrete-to-teflon friction coefficient is taken equal to 0.001.

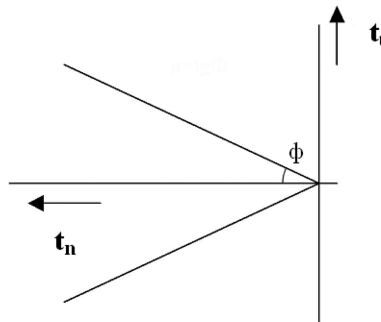


Fig. 4 Frictional behaviour of the joint

### 3.2 Material model

Concrete can be considered an elastic material only for a small stress range. While the level of compression stresses in the joints is very low, concrete can be modelled in compression as an elastic and linear material, with a deformation modulus  $E_c=28000$  MPa and a Poisson coefficient  $\nu=0.2$ .

In order to reproduce the behaviour of the panels before failure, some smeared crack models were applied to simulate the cracking of the keys in the lateral panel. These models did not work properly, since the response imperceptibly separated from the linear behaviour, permitting the load to grow indefinitely, and showing no sensibility to the artificial reductions of the tensile strength. Cracking did appear in the modelled keys, but was unable to reach the capacity of the panel. Apparently, so many sources of non linearity did not allow the code to reach a reasonable result. Hence, modelling of the cracking of the concrete was eventually abandoned, as it was not considered crucial. Indeed, it is to highlight that the failure mode observed on panels is radically different than that observed in experimental tests on scaled girders. In the case of panels, cracking is vertical and the keys fail in the plane of the joint. In the case of girders, it is a diagonal cracking that induces failure, starting at the joint and progressing across the segment. During beam tests (Turmo *et al.* 2006b, Aparicio *et al.* 2001, Ramirez 1989), joints present an elastic behaviour and the keys maintain their integrity during failure. As the main target of this research is to provide a joint model able to model actual bridges, to keep an elastic material model for concrete was considered sufficient for the purpose of this research. It is clear than more sophisticated material models could be used taking into account some other non linear phenomena (Dujc *et al.* 2010, Lee *et al.* 2010, Gamino *et al.* 2010, Cagatay and Dincer 2011) in the future for modelling the behaviour of the panels up to failure.

### 3.3 Modelling of the panels

Four types of panels were numerically tested. Symmetry was systematically applied to favour the convergence of the non-linear calculation. The analysis was performed in two dimensions.

Keys and joints were modelled with their real geometry. Due to the stress gradients developed in the keys, it was necessary to assure that the stress distribution could be at least linear within the elements. Since for irregular element geometries lagrangian elements of nine nodes behave better than quadratic serendipitic elements (Zienkiewicz and Taylor 1994), flat tension elements of 9 nodes and 18 degrees of freedom were used for modelling the concrete. The contact between sub-panels was modelled using 3-node interface elements.

The number of elements used in the modelling varied for each panel. As an example, Fig. 5 shows the mesh used to model the open joint test (PC-JA). The model had 1165 elements and 9406 degrees of freedom. The mesh detail of the keys, common for all the tests, is shown in Fig. 6.

Panels were loaded by a point-force acting in the upper part. A rigid plate between the load and the panel was modelled to distribute the load along the application surface. The support plates of the panels, with the corresponding rollers, are simulated through a rigid plate where the vertical movements are blocked only at one of its points so that the support can rotate and displace horizontally. The prestressing was introduced as external forces acting at the anchorages. The evolution of the prestressing in the numerical test was identical to the evolution of the prestressing forces measured with the load cells during the experimental tests.

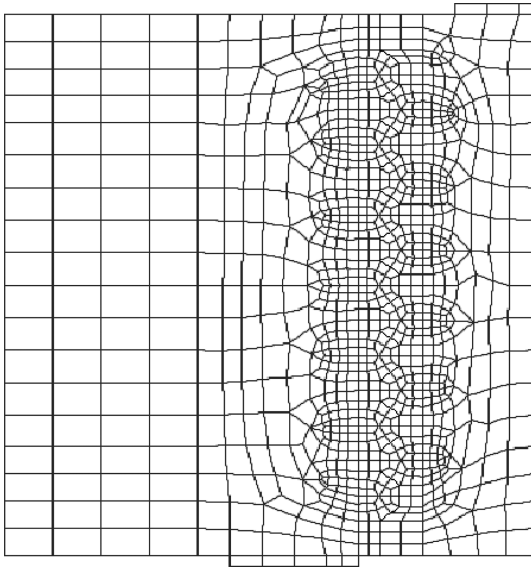


Fig. 5 Mesh used to model the open joint test

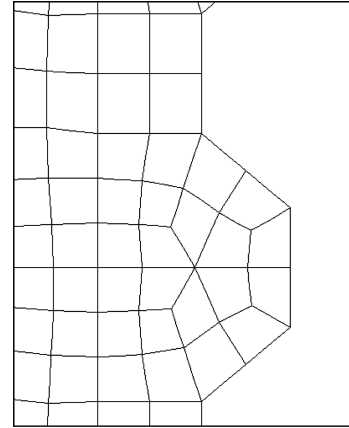


Fig. 6 Key mesh detail

### 3.4 Analysis

The analysis of the panels has been accomplished using the finite elements code Diana 8.1, developed by TNO Building and Construction Research. It is a commercial program based on the displacement method (DIANA, DIplacement method ANALyser), that permits physical and geometrical non-linear analysis.

A Gauss integration with a  $3 \times 3$  scheme was used for the lagrangian elements. A nodal lumping scheme was used when integrating interface elements; one integration point for each pair of nodes. For interface elements, a Gaussian integration scheme may lead to unacceptable oscillations in the results (Diana 2002).

Failure was reached in twenty-three steps in all panels. Equilibrium was reached in each step after successive iterations applying the Newton-Raphson method.

### 3.5 Analysis of the results

#### 3.5.1 Friction tests

In the friction test, the material has been considered elastic and linear. The nonlinearity of the analysis is concentrated in the joint.

Figs. 7 and 8 show the correlation between the results of the numerical analysis (FEM) and the experimental tests (TEST). In Fig. 7, which shows the load-deflection diagram, a good correlation between the numerical and experimental results can be observed. Fig. 8 shows the evolution of the slipping of the joint in three points located at different heights of the panel as a function of the load level. The slipping begins in the upper zone, where normal stresses are smaller, and progresses toward the lower part of the joint. Then, failure occurs when the upper part of the joint has accumulated a certain slipping.

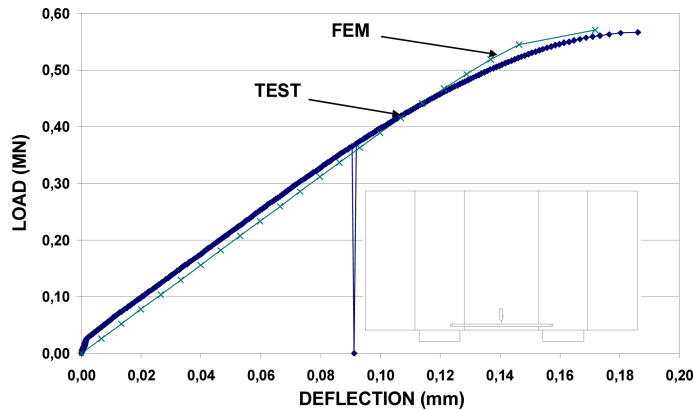


Fig. 7 Load-deflection diagram for PC-R-2 test

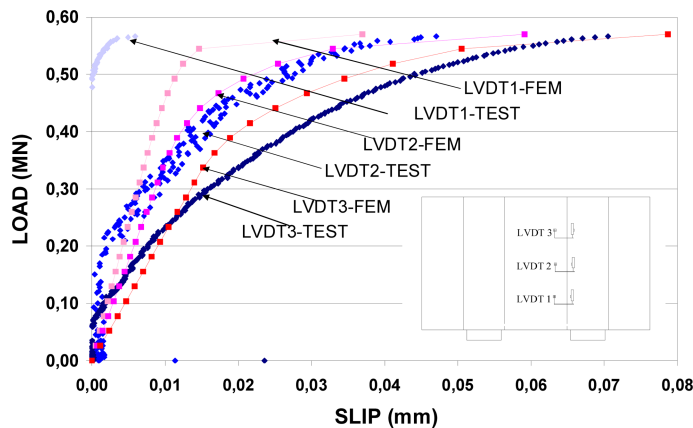


Fig. 8 Load-slip curves in PC-R-2 test

The shear capacity of the joint,  $V_u$ , depends on the friction coefficient,  $\mu_1$ , and on the normal stress,  $\sigma_n$ .

$$V_u = \int_A \mu_1 \cdot \sigma_n dA \quad (3)$$

The friction coefficient,  $\mu_1$ , quantifies the resistance against slipping generated when the irregularities and protuberances of a surface penetrates between the irregularities and protuberances of another surface, when they are in contact and compressed, and one surface attempts to displace against the other. Hence, this coefficient depends on the degree of smoothness of the surfaces. Tests show that the smoothness of the joint surface increases when slipping occurs; like a polishing effect that slightly reduces  $\mu_1$  when slipping takes place (Foure *et al.* 1993). The fact that the upper part of the joint has already slipped before the ultimate load is reached, contradicts the hypothesis of a strict uniformity of the friction coefficient in all the points of the surface.

If an exact calculation is required, or if the surface of the panel is large enough to accumulate an important slipping, it would be necessary to consider the variation of the friction coefficient as a function of the joint slipping to evaluate the shear capacity of the panel. However, for the conditions of

these tests, it seems reasonable to consider the friction coefficient as a constant, which leads to Eq. (4).

$$V_u = \int_A \mu_1 \cdot \sigma_n dA \approx \mu_1 \int_A \sigma_n dA = \mu_1 \cdot N \quad (4)$$

where a constant magnitude of the friction coefficient,  $\mu_1$ , between concrete surfaces has been considered, independently of the area and of the existing normal stress.

### 3.5.2 Cohesion tests

Fig. 9 shows the mesh used in the numerical modelling of PC-C and SFRC-C tests. It is worth noting that interface elements (in black) have been placed to model the behaviour of the neoprene-teflon sheets (vertical elements) and the contact surfaces between the keys (inclined elements). Thus, the separation between the faces of the joint has been simulated by establishing dependency relationships only between the degrees of freedom of the surfaces in touch, those simulated by interface elements. When introducing the initial prestressing force, the interface elements of the keys are not loaded. Only the neoprene sheet counterbalances the prestressing.

The load-deflection responses obtained from the experimental cohesion tests are shown in Fig. 10 (TEST), where a notable stiffness variation among the tests can be appreciated. In the first numerical test (PC-C-FEM-1), a continuous contact between the keys was considered. In order to do so, parameters  $k_n$  and  $k_t$  adopted the penalty values defined in Table 2. The results obtained with this configuration were excessively rigid (PC-C-FEM-1 in Fig. 10). However, since the surfaces of the joint are in contact, the hypothesis of a much more flexible behaviour was considered in the second numerical test (PC-C-FEM-2). Usually, high penalty values are used in contact and interface elements intending to simulate either the initial continuous geometry before the decompression or the high resistance to penetration of two hard different surfaces, whereas this lower stiffness attempts to simulate the contact of two concrete surfaces in a more realistic way. When two concrete surfaces make contact, they connect through the contact of the different irregularities of their surfaces. For growing compression stresses, these irregularities deform (crushing), imposing a

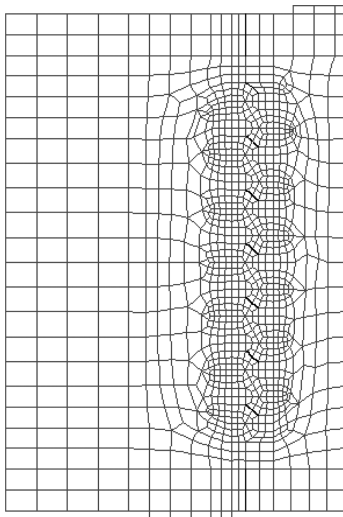


Fig. 9 Mesh used to model cohesion tests

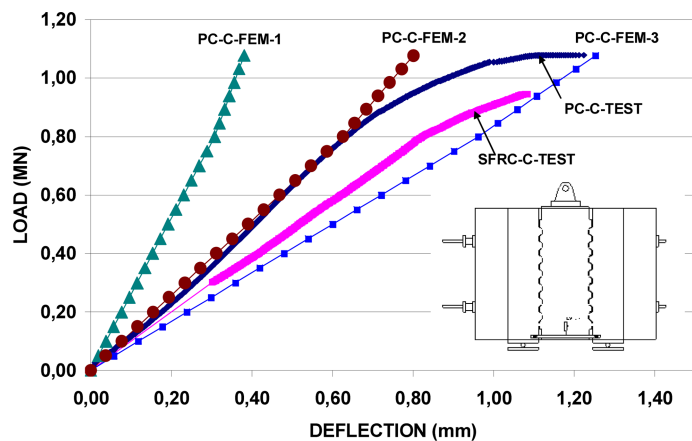


Fig. 10 Load-deflection diagram for cohesion test

Table 3 Different normal stiffness constants  $k_n$ , adopted to model a concrete dry joint

Test	$k_n$ (MN/m <sup>3</sup> )
PC-C-FEM-1	10000000
PC-C-FEM-2	50000
PC-C-FEM-3	25000

relative approximation between the two faces. The faces of the joint approached 0.3 mm when a prestressing force  $Q_u = 0.9$  MN was applied in PC-C-FEM-2 test (which leads to a mean compressive stress,  $\sigma_{nm} = 15$  MPa between the surfaces in contact). The approximation was 0.6 mm under similar normal stresses in PC-C-FEM-3 test. A summary of the  $k_n$  coefficients used in the stiffness matrix to link normal stresses and relative displacement in the joints is presented in Table 3.

The crushing phenomenon of the irregularities of the joints faces would explain the difference in stiffness between the first numerical test PC-C-FEM-1 and the experimental results. This phenomenon not only leads to different displacement results, but also modifies the stress field.

Fig. 11 shows the relationship between the applied load and the shear stresses in each key for the PC-C-FEM-1 test. These shear stresses have been calculated numerically integrating the normal stresses,  $t_n$ , and tangential stresses,  $t_t$ , acting in each joint. The forces calculated in this way are projected on a vertical axis and divided by the resistant area of the key  $A_{ki}$ . Fig. 11 shows how the shear load distribution is not uniform throughout the height of the joint, being the shear flow concentrated in the extreme keys. The most loaded key is the upper one (key 1 in Fig. 11), followed by the bottom key (key 7). It can be observed that the stress distribution along the joint is quite unequal, with the upper key transferring three times more load than the intermediate keys. In the case of PC-C-FEM-2 test, Fig. 12, a much more uniform stress distribution can be observed, with the most loaded upper key sustaining 1.5 times more load than the central keys. This relationship decreases to 1.25 in the case of PC-C-FEM-3 test. These results can be also checked comparing Fig. 13 (from the analysis of PC-C-FEM-1) and Fig. 14 (from PC-C-FEM-2), the later showing a more uniform shear stress distribution.

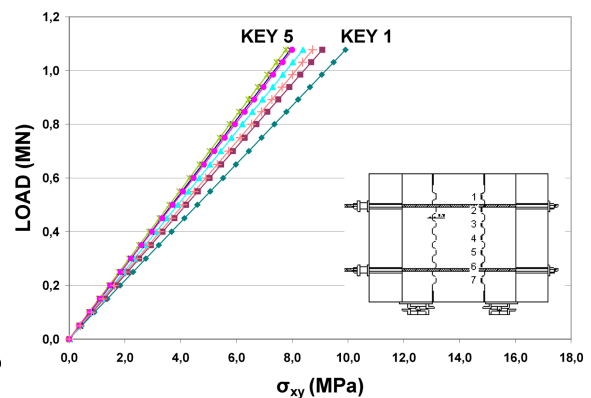
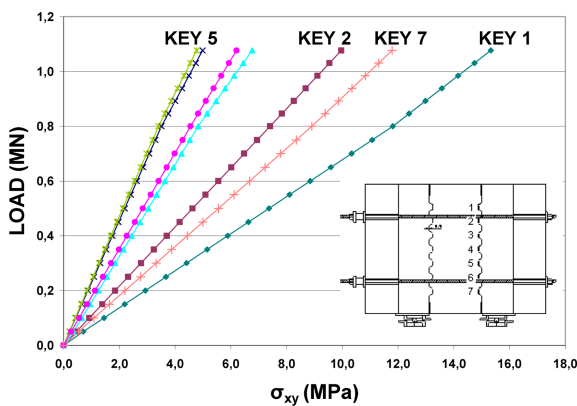


Fig. 11 Load-shear stress response of keys in PC-C-FEM-1 test

Fig. 12 Load-shear stress response of keys in PC-C-FEM-2 test

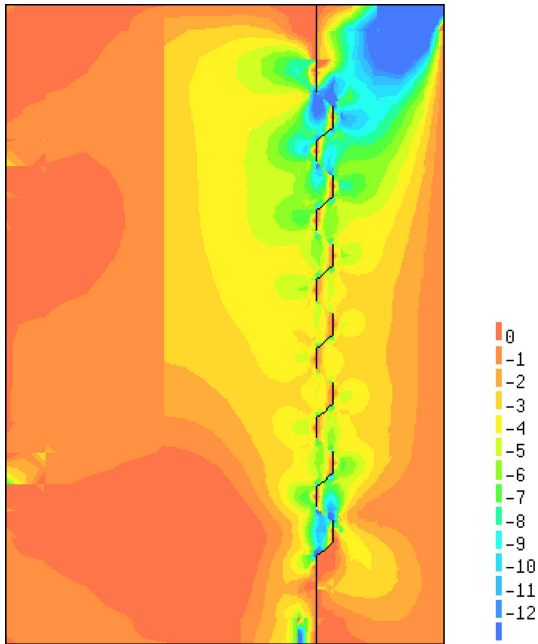


Fig. 13 Shear stress distribution (MPa) in PC-C-FEM-1 test under maximum load

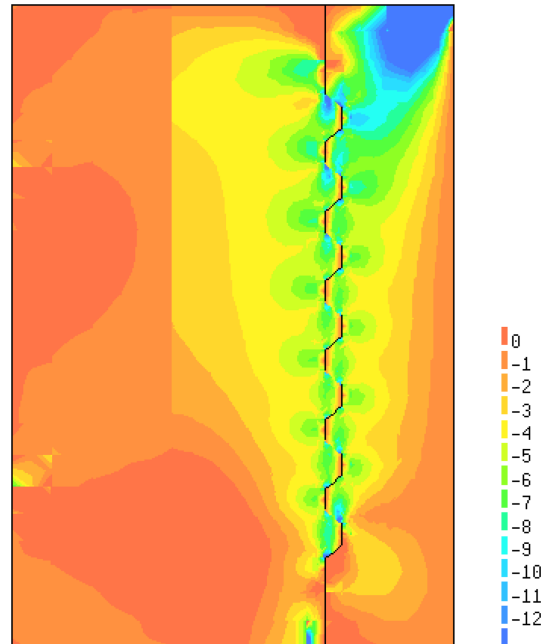


Fig. 14 Shear stress distribution (MPa) in PC-C-FEM-2 test under maximum load

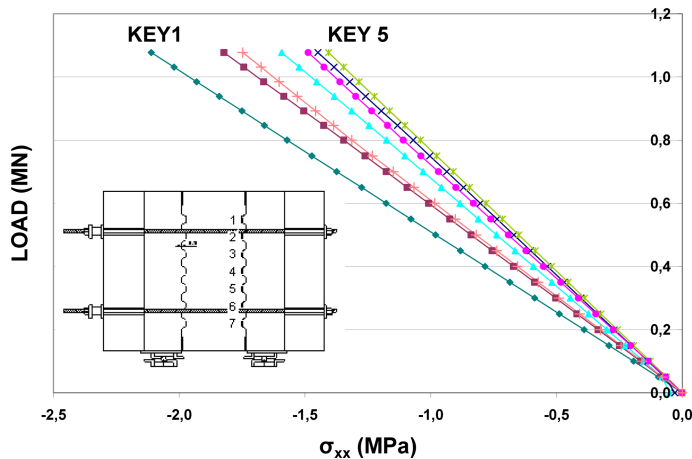


Fig. 15 Load-compressive stress response of keys in PC-C-FEM-3 test

Shear transfer in a joint with several keys is somehow analogous to the elastic force transfer in a lap joint with several bolts. Depending on the stiffness of the bolts, shear is transferred in a different way. If very stiff fasteners are provided, the shear flow will concentrate in the extreme bolts. On the other hand, flexible fasteners will lead to an equally distributed shear transfer among the bolts.

This is of great importance for the safety and for the global strength of dry joints. Being the shear keys un-reinforced and being the concrete a brittle material in shear and tension, little plastic redistribution of shear stresses can be expected at ultimate loads. This means that if the distribution

of shear stresses is even all the keys will reach their ultimate shear capacity at the same external load level, being the shear strength of the joint the addition of the individual capacity of each key. On the other hand, if the shear stress distribution were concentrated in the two extreme keys, these introduce would between these and failed when they reached their ultimate shear capacity, and transferred their load to the subsequent keys, being the global shear strength of the joint significantly reduced.

Other result that comes out from the analysis is that the horizontal projection of the stresses transmitted through the interface elements induces compressive stresses in the key. In spite of considering in the design of the test that the horizontal component of the stresses at key level would be nil, the special geometry of the key causes the shear flow to entail the transmission of normal stresses. Fig. 15 shows the compressive stress in each key from PC-C-FEM-2 test, where a value of 2.0 MPa is reached in the most loaded key.

### 3.5.3 Closed joint tests

The sensibility of the numerical simulation with regard to the normal stiffness,  $k_n$ , of the joint was again evaluated in the closed joint tests. The joints were modelled using the  $k_n$  values of Table 3; tests PC-JC-FEM-1, PC-JC-FEM-2 and PC-JC-FEM-3. Fig. 16 shows the mesh used in the analysis.

Fig. 17 presents a comparison between the load-deflection curves from PC-JC and SFRC-JC tests and those obtained in the numerical analysis. Firstly, it is worth to emphasize that the numerical tests PC-JC-FEM-2 and PC-JC-FEM-3 resulted highly unstable at low load levels, not achieving convergence even when the step was reduced and the number of iterations increased. Secondly, it was observed that the deflection results are highly dependent on the stiffness of the joint element used in the analysis,  $k_n$ . In this sense, test results are better estimated with lower values of  $k_n$ .

In terms of stress distribution, results are similar; the contribution of each key to the shear transfer

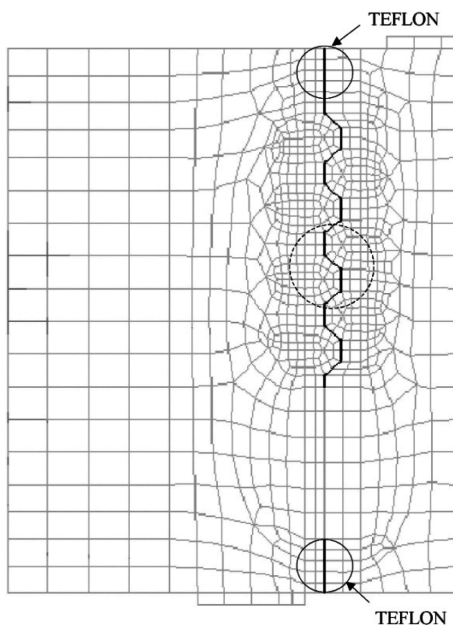


Fig. 16 Mesh used to model closed joint tests

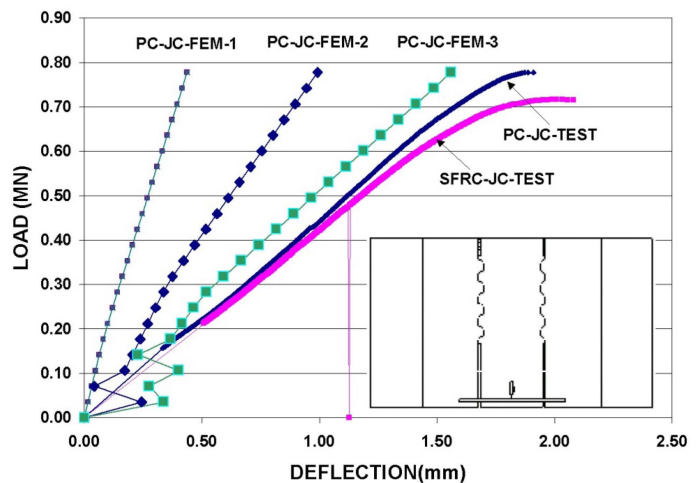


Fig. 17 Load-deflection diagram for closed joint tests

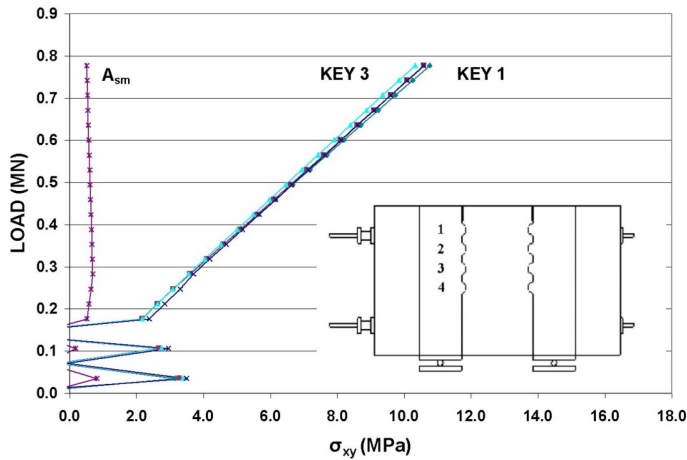


Fig. 18 Load-shear stress response of keys in PC-JC-FEM-3 test

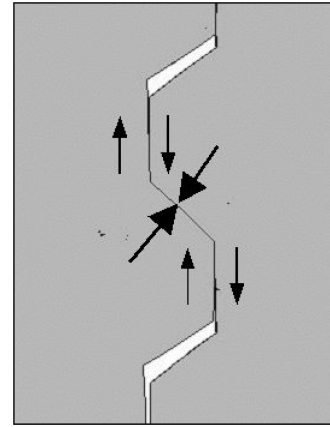


Fig. 19 Detail of key displacement in PC-JC-FEM-3 test

does not significantly depend on  $k_n$ . This can again be explained with the bolted lap joint analogy. In an elastic analysis of a bolted lap joint, the higher is the number of bolts in the joint, higher is the difference among the shear transferred by each bolt. Differences between the shear transferred by each key in 7-key joints (cohesion tests) are higher than in 4-key joints (closed joint tests). Fig. 18 shows the evolution of the mean shear stress within each key, and at the smooth zones between keys ( $A_{sm}$ ), as a function of the load level. The contribution of each key to the shear flow is practically identical and independent of their location. It is worth to emphasize that for the actual level of normal stresses reached in these tests ( $\sigma_n \approx 2$  MPa), the contribution of the keys to the transference of shear stress is significantly greater than the contribution of the smooth zone between the keys of the joint, the former being practically constant throughout the entire test. In fact, the numerical study shows that the slipping between the joint faces is produced in the first load steps. Then, the smooth zones  $A_{sm}$  cannot transfer more shear stress than that of the initial stage. From this moment on, it is the support action of the key that absorbs the load increase. A detail of the displaced geometry after slipping is shown in Fig. 19 for PC-JC-FEM-3 test.

The relative importance of the stress transmitted by the keys ( $A_k$ ), with respect to the stress transmitted by the smooth area ( $A_{sm}$ ) is significant. According to these numerical tests, about a 95% of the ultimate shear is transmitted through the keys.

#### 3.5.4 Open joint tests

Due to the small lever arm available to counterbalance flexure with this configuration, and due to the important opening of the joint observed during the tests, a geometrically non linear analysis was performed. In this manner, the geometry was updated in every iteration as a function of the displacements obtained in the previous iteration.

Three linear constitutive laws of the interface have been considered for the modelling, Table 3 (PC-JA-FEM-1, PC-JA-FEM-2 and PC-JA-FEM-3 tests). Concrete was considered elastic and linear. The characteristics of the key contact between sub-panels observed in the experimental tests were reproduced in the numerical tests. Fig. 20 shows the condition of the geometry in test PC-JA-FEM-2 at maximum load, where only keys 1, 2 and 3 are in contact. It is to highlight that key 3 is

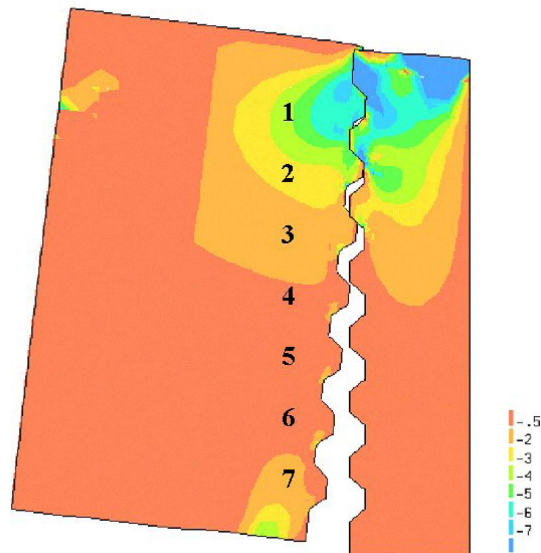


Fig. 20 Shear stress distribution (MPa) in PC-JA-FEM-2 test under maximum load

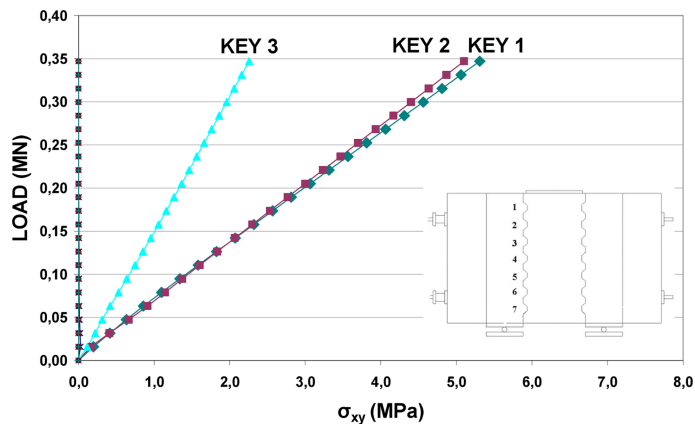


Fig. 21 Load-shear stress response of keys in PC-JA-FEM-1 test

below the neutral axis.

The evolution of the mean shear stress within each key and at the smooth zones between keys ( $A_{sm}$ ) in function of the load level is presented in Fig. 21 (PC-JA-FEM-1) and Fig. 22 (PC-JA-FEM-3). Shear stress distribution between keys 1 and 2 becomes uniform when reducing the stiffness  $k_n$  of the joint. The first key just below the neutral axis, key 3, carries a lower shear stress than the preceding upper keys. The rest of the keys do not transfer any load.

The contribution of the different keys to the shear flow (keys 1, 2 and 3 in Fig. 18) and the contribution of the smooth area of the joint ( $A_{sm}$ ) obtained in the numerical tests, are summarized in Table 4. In this case, the fact that high compressive stresses are concentrated in the smooth zone above the keys due to flexure causes a relatively higher shear transfer across this zone than that observed in the closed joint tests.

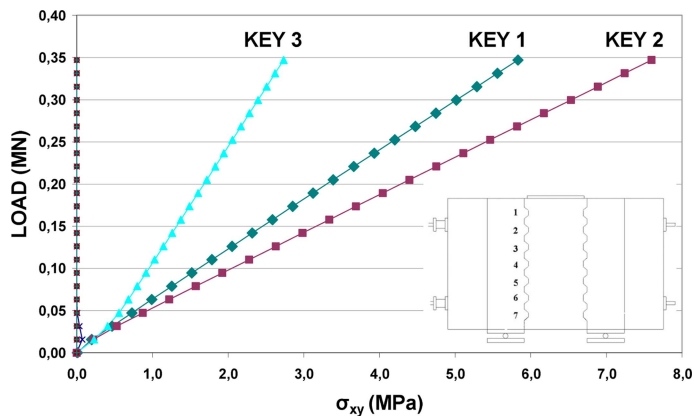


Fig. 22 Load-shear stress response of keys in PC-JA-FEM-3 test

Table 4 Contribution to shear transfer of keys ( $A_{k1}$ ,  $A_{k2}$  y  $A_{k3}$ ) and smooth area of the joint  $A_{sm}$  in open joint tests

		$V_u$ (MN)	%	$V_u$ (MN)	%	$V_u$ (MN)	%
PC-JA-FEM-1	$A_{k1}$	0,052	30,11	0,145	83,45	0,174	100,00
	$A_{k2}$	0,068	39,23				
	$A_{k3}$	0,025	14,12				
	$A_{sm}$	0,029	16,55	0,029	16,55		
PC-JA-FEM-2	$A_{k1}$	0,046	26,51	0,113	65,39	0,174	100,00
	$A_{k2}$	0,047	26,96				
	$A_{k3}$	0,021	11,92				
	$A_{sm}$	0,060	34,61	0,060	34,61		
PC-JA-FEM-3	$A_{k1}$	0,048	27,61	0,114	65,87	0,174	100,00
	$A_{k2}$	0,046	26,52				
	$A_{k3}$	0,020	11,74				
	$A_{sm}$	0,059	34,13	0,059	34,13		

#### 4. Conclusions

A joint model that reproduces the experimental test behaviour of eight panel tests in the elastic phase has been validated. As failure of externally prestressed precast segmental structures never occurs in the joint plane, this model will be useful for the modelling of such real structures up to failure. Several conclusions have been reached regarding the application of the model to the analysis of the panel tests:

(1) When modelling the behaviour of the joint, it is fundamental to adequately reproduce the physical phenomenon that takes place when two concrete surfaces make contact. When two concrete elements are in touch, they connect through the contact of the different irregularities of their surfaces. For growing compression stresses, these irregularities deform (crushing), imposing a relative approximation between the two concrete faces. This phenomenon is modelled adopting an adequate axial stiffness

coefficient in the joint,  $k_n$ . Experimental test results were better approximated with  $k_n$  values ranging from 25000 to 50000 MN/m<sup>3</sup>.

(2) Considering the contribution of the different mechanisms (friction and direct bearing of the keys) to the overall shear force transference, the supporting action of the keys prevails over friction. When shear keys in contact exist in the joint, their contribution to the shear transfer is greater than that of smooth area between keys.

(3) Regarding the behaviour of the smooth zones between keys, it is worth to denote that slipping between concrete faces is not sudden, but develops in a progressive manner. The less compressed contact zones resist lower shear stresses and consequently are the first to slide. This microslippings, produced where the friction resistance is lower, are accumulated until the last point of the compressed area slips. At that point, the entire joint slides in a notorious manner.

(4) With respect to the behaviour of the shear keys, a quite uniform stress distribution within the keys is verified. In the experimental tests, all the keys contribute in a very similar way to the shear transfer, independently of its position. This is due to the fact that the axial stiffness coefficient of the surfaces in contact,  $k_n$ , does not correspond to that of a continuous medium, but to a flexible one.

## Acknowledgements

The authors wish to thank the support provided by the Ministerio de Ciencia e Innovacion and by the Junta de Comunidades de Castilla-La Mancha (Spain) through the research projects BIA2009-13056 and PII2I09-0129-4085, directed by Jose Turmo.

## References

- AASHTO (2010), *AASHTO LRFD Bridge design specifications, 5th Edition, with 2010 Interim Revisions*, AASHTO, Washington.
- Aparicio, A.C., Ramos, G. and Casas, J.R. (2001), "Testing of externally prestressed concrete beams", *Eng. Struct.*, **24**(2), 73-84.
- Au, F.T.K., Chan, K.H.E., Kwan, A.K.H. and Du, J.S. (2009), "Flexural ductility of prestressed concrete beams with unbonded tendons", *Comput. Concrete*, **6**(6), 451-472.
- Beattie, S.M., Buyukozturk, O. and Bakhoum, M.M. (1989), *Structural behavior improvements in joints of PCSB through the use of steel fibers R03-89*, Civil Engineering Department, MIT, Cambridge.
- Brockmann, C. and Rogenhofer, H. (2000), "Bang Na Expressway, Bangkok, Thailand - World's longest bridge and largest precasting operation", *J. Prest. Concrete Inst.*, **45**(1), 26-38.
- Buyukozturk, O., Bakhoum, M.M. and Beattie, S.M. (1990), "Shear behavior of joints in precast concrete segmental bridges", *J. Struct. Eng.-ASCE*, **116**(12), 3380-3401.
- Cagatay, I.H. and Dincer, R. (2011), "Modeling of concrete containing steel fibers: toughness and mechanical properties", *Comput. Concrete*, **8**(3), 357-369.
- DIANA (2002), *User's manual. Element Library*. TNO, Delft.
- Dujc, J., Brank, B., Ibrahimbegovic, A. and Brancherie, D. (2010), "An embedded crack model for failure analysis of concrete solids", *Comput. Concrete*, **7**(4), 331-346.
- Foure, B., Bouafia, Y., Soubret, R. and Thomas, P. (1993), "Shear test on keyed joints between precast segments", *Proceedings of the Workshop AFPC External Prestressing in Structures*, Saint-Rémy-lès-Chevreuse.
- Gamino, A.L., Manzoli, O.L., Antunes de Oliveira e Sousa, J.L. and Nogueira Bittencourt, T. (2010), "2D evaluation of crack openings using smeared and embedded crack models", *Comput. Concrete*, **7**(6), 483-

- 496.
- Huang, J. and Eibl, J. (1993), "Design of segmental bridges under combined bending, shear and torsion. FE-study", *Proceedings of the Workshop AFPC External Prestressing in Structures*, Saint-Rémy-lès-Chevreuse.
- Issa, M.A. (2007), "Structural behavior of single key joints in precast concrete segmental bridges", *ASCE J. Bridge Eng.*, **12**(3), 315-324.
- Kamaitis, Z. (2008), "Field investigation of joints in precast post-tensioned segmental concrete bridges", *Baltic J. Road Bridge Eng.*, **3**(4), 198-205.
- Koseki, K. and Breen, J. (1983), *Exploratory study of shear strength of joints for precast segmental bridges*, Texas State Department of Highways and Public Transportation
- Lee, B.Y., Kim, J.K. and Kim, Y.Y. (2010), "Prediction of ECC tensile stress-strain curves based on modified fiber bridging relations considering fiber distribution characteristics", *Comput. Concrete*, **7**(5), 455-468.
- Megally, S., Seible, F. and Dowell, R.K. (2003a), "Seismic performance of precast segmental bridges: Segment-to-segment joints subjected to high flexural moments and low shears", *PCI J.*, **48**(2), 80-96.
- Megally, S., Seible, F. and Dowell, R.K. (2003b), "Seismic performance of precast segmental bridges: Segment-to-segment joints subjected to high flexural moments and high shears", *PCI J.*, **48**(3), 72-90.
- Muller, J. (1980), "Construction of the long key bridge", *J. Prestressed Concrete Inst.*, **25**(6), 97-111.
- Muller, J. and Gauthier, Y. (1990), "Ultimate behaviour of precast segmental box girders with external tendons", *External Prestressing in Bridges*, ACI-SP-120, Detroit.
- Naaman, A.E. (1990), "A new methodology for the analysis of beams prestressed with external or unbonded tendons", *Ext. Prestressing in Bridges*, ACI-SP-120, Detroit.
- Ramirez Aguilera, G. (1989), *Behavior of unbonded post-tensioning segmental beams with multiple shear keys*, Master Thesis, University of Texas at Austin.
- Ramos, G. and Aparicio, A.C. (1996), "Ultimate analysis of monolithic and segmental externally prestressed concrete bridges", *ASCE J. Bridge Eng.*, **1**(1), 10-18.
- Ramirez, G., MacGregor, R.J.G., Kreger, M.E., Roberts-Wollmann, C.L. and Breen, J.E. (1993), "Shear strength of segmental structures", *Proceedings of the Workshop AFPC External Prestressing in Structures*, Saint-Rémy-lès-Chevreuse.
- Rezende, P.C. (1989), *Modelisation du comportement jusqu'à la rupture en flexion de poutres en béton a précontrainte extérieure ou mixte*, Ph.D. Thesis, Ecole Centrale, Paris.
- Rombach, G.A. (2004), "Dry joint behavior of hollow box girder segmental bridges", *Proceedings of the International Fib Symposium – Segmental Construction in Concrete*, FIB, New Delhi.
- Rombach, G.A. and Abende, R. (2008), "Bow-shaped segments in precast segmental bridges", *Eng. Struct.*, **30**(6), 1711-1719.
- Rombach, G.A. and Specker, A. (1999), "Numerical modelling of segmental bridges", *Proceedings of the European Conference on Computational Mechanics*, W.Wunderlich, ed., Munich, Germany.
- Rombach, G.A. and Specker, A. (2000), "Finite element analysis of externally prestressed segmental bridges", *Proceedings of the Fourteenth Engineering Mechanics Conference*, ASCE, Austin, Texas.
- Takebayashi, T., Deeprasertwong, K. and Leung, Y. (1994), "A full-scale destructive test of a precast segmental box girder bridge with dry joints and external tendons", *P. I. Civil Eng.-Str. B.*, **104**(3), 297-315.
- Turmo, J. (2003), *Flexure and shear behavior of segmental concrete bridges with external prestressing and dry joints*, PhD Thesis, Universitat Politècnica de Catalunya, BarcelonaTech, July.
- Turmo, J., Ramos, G. and Aparicio, A.C. (2005), "FEM study on the structural behaviour of segmental concrete bridges with unbonded prestressing and dry joints: Simply supported bridges", *Eng. Struct.*, **27**(11), 1652-1661.
- Turmo, J., Ramos, G. and Aparicio, A.C. (2006a), "Shear strength of dry joints of concrete panels with and without steel fibres. Application to precast segmental bridges", *Eng. Struct.*, **28**(1), 23-33.
- Turmo, J., Ramos, G. and Aparicio, A.C. (2006b), "Shear behaviour of unbonded post-tensioned segmental beams with dry joints", *ACI Struct. J.*, **103**(3), 409-417.
- Turmo, J., Ramos, G. and Aparicio, A.C. (2006c), "FEM modelling of unbonded post-tensioned segmental beams with dry joints", *Eng. Struct.*, **28**(13), 1852-1863.
- Turmo, J., Ramos, G. and Aparicio, A.C. (2011), "Structural behaviour of segmental concrete continuous bridges with unbonded prestressing and dry joints", *Struct. Infrastruct. E.*, **7**(11), 857-868.
- Vonganan, B. (1997), *Effect of external tendon layout on flexural behaviour of precast segmental box girder*

*bridges*, Thesis University Innsbruck.

Zhou, X., Mickleborough, N. and Li, Z. (2005), "Shear strength of joints in precast concrete segmental bridges", *ACI Struct. J.*, **102**(1), 3-11.

Zienkiewicz, O.C. and Taylor, R.L. (1994), *Finite element method. basic formulas and linear problems*, CIMNE, Barcelona.

CC